Applied Mathematics and Computation 259 (2015) 838–857

Contents lists available at ScienceDirect

Applied Mathematics and Computation

journal homepage: www.elsevier.com/locate/amc

Local thermal non-equilibrium effects on thermal convection in a rotating anisotropic porous layer

I.S. Shivakumara [a,*], A.L. Mamatha [b], M. Ravisha [c]

[a] Department of Mathematics, Bangalore University, Bangalore 560001, India
[b] Department of Mathematics, Smt. Rukmini Shedthi Memorial National Government First Grade College, Barkur 576210, India
[c] Department of Mathematics, Dr. G. Shankar Government Women's First Grade College and Post Graduate Study Centre, Ajjarakadu, Udupi 576101, India

ARTICLE INFO

Keywords:
Anisotropy
Local thermal non-equilibrium (LTNE)
Convection
Rotation
Darcy model

ABSTRACT

Effects of local thermal non-equilibrium (LTNE) on thermal convection in a rotating fluid-saturated anisotropic porous layer are investigated. The analysis has been carried out by constructing a simplified model consisting of six coupled nonlinear ordinary differential equations. The study reveals the equivalence of linear and nonlinear stability boundaries indicating the linearized instability theory captures completely the physics of the onset of convection. Results show that the presence of rotation is to introduce oscillatory convection once the Taylor number exceeds a threshold value. The preferred mode of instability is found to be influenced significantly by the mechanical anisotropy parameter as well and it is demonstrated that it has both stabilizing and destabilizing effects on the steady onset in the presence of rotation. Besides, asymptotic analyses for small and large values of the interphase heat transfer coefficient are presented. Heat transport is calculated in terms of Nusselt number. Also, the coupled nonlinear ordinary differential equations are solved numerically using Runge–Kutta method and the transient behavior of Nusselt number is demonstrated for various values of physical parameters.

1. Introduction

Buoyancy driven convection in a layer of porous medium heated from below using a local thermal non-equilibrium (LTNE) model has received considerable attention of researchers in the recent past because of its numerous applications in different fields of science and engineering such as tube refrigerators in space, nanofluid flows, fuel cells, resin flow, processing of composite materials, flows in microchannels, nuclear reactor maintenance, heat exchangers, flow in porous metallic foams, convection in stellar atmospheres to mention a few (Virto et al. [1], Straughan [2] and references therein). In particular, thermal instability in porous media using LTNE effects was considered by Banu and Rees [3] and Malashetty et al. [4]. By performing the global nonlinear stability analysis on the problem, Straughan [5] demonstrated the equivalence of linear and nonlinear stability limits. The growing volume of work devoted to this area of research has been reviewed extensively and well documented in the literature [6–9].

Majority of the investigations on LTNE free convection in porous media have been dealt with isotropic porous materials. However, most porous media encountered in nature and in industry are anisotropic in their mechanical and thermal properties. Anisotropy is particularly important in a geological context, because sedimentary rocks generally have a layered

* Corresponding author.
E-mail addresses: shivakumarais@gmail.com (I.S. Shivakumara), ravishmamatha@gmail.com (M. Ravisha).

http://dx.doi.org/10.1016/j.amc.2015.03.023
0096-3003/

structure; the permeability in the vertical direction is often much less than in the horizontal direction. Anisotropy can also be a characteristic of artificial porous materials like pelletting used in chemical engineering process and fiber material used in insulating purpose. Furthermore, thermal conductivity of many sedimentary and metamorphic rocks is strongly anisotropic, and lateral heat flow will be significant in such situations. Anisotropy effects in general have been reviewed by McKibbin [10,11] and Storesletten [12,13]. Malashetty et al. [14] examined analytically the effect of anisotropy in permeability as well as thermal diffusivities on the onset of convection in a porous medium using a LTNE model. Shivakumara et al. [15] investigated the effects of boundary and local thermal non-equilibrium on the criterion for the onset of convection in a sparsely packed horizontal anisotropic porous layer.

The effect of rotation expressed as a Coriolis force plays a vital role on the onset of convection in porous media because of its natural occurrence as well as its utility in control of convection in many technological problems. Qin and Kaloni [16] studied the effect of rotation on nonlinear thermal convection in a porous medium. Vadasz [17] used linear and weak non-linear stability theories to study the effect of Coriolis force on gravity-driven convection in a rotating porous layer heated from below by employing the modified Darcy model. The differences as well as similarities between the porous medium and pure fluids convection results are highlighted in this study. An excellent review of research on thermal convection in a rotating porous medium has been given by Vadasz [18]. A nonlinear stability analysis for thermal convection in a rotating porous layer has been performed by Straughan [19] while the effect of LTNE on such a study has been discussed by Straughan [5]. Govender [20] analyzed the effect of Coriolis force on centrifugally driven convection in a rotating layer of porous medium. Malashetty et al. [21] studied linear and nonlinear thermal convection in a rotating porous layer using a thermal non-equilibrium model. Shivakumara et al. [22] investigated the effect of Coriolis force on linear and nonlinear thermal convection in a layer of rotating porous medium using the Brinkman–Lapwood–Darcy model with fluid viscosity different from Brinkman viscosity and uncovered the dual behavior of permeability and ratio of viscosities on the onset of stationary convection under certain conditions. The inertia effects on thermal convection in a horizontal layer of rotating Darcy porous medium has been considered by Falsaperla et al. [23]. A limited number of studies have also been dealt with the effect of anisotropy on convective instability in a rotating porous layer. Govender [24] studied onset of convection in an anisotropic porous layer subject to centrifugal body force using the Darcy model, while Govender and Vadasz [25] investigated the effect of mechanical and thermal anisotropies on the linear stability of stationary convection in rotating porous media. The details are well documented in the book by Nield and Bejan [9]

The main objective of the present paper is to study the combined effects of inertia and LTNE on linear and nonlinear thermal convection in a rotating anisotropic porous layer heated from below. Both mechanical and thermal anisotropies are considered. A simplified model is introduced to construct a system of autonomous nonlinear ordinary differential equations with the properties that the linear theory and the finite amplitude solutions obtained up to second order in the amplitude expansion, are identical to those obtained in the case of full problem. Besides, the nonlinear system of finite amplitude equations is solved numerically using Runge–Kutta method to know the transient behavior of Nusselt number.

2. Mathematical formulation

We consider an incompressible fluid-saturated horizontal anisotropic porous layer of thickness d rotating with an angular velocity $\vec{\Omega} = (0, 0, \Omega)$ about the vertical axis. A Cartesian coordinate system (x, y, z) is chosen such that the origin is at the bottom of the porous layer and the z- direction is denoted by the vector $\hat{k}$ with $(\hat{i}, \hat{j}, \hat{k})$ being the standard basis. Gravity acts in the negative z-direction. The lower and upper surfaces of the anisotropic porous layer are held fixed at constant temperatures T_l and T_u ($<T_l$) respectively. The basic equations are:

$$\nabla.\vec{q} = 0, \tag{2.1}$$

$$\frac{\rho_0}{\varepsilon}\frac{\partial \vec{q}}{\partial t} = -\nabla p - \frac{2\rho_0}{\varepsilon}(\vec{\Omega}\times\vec{q}) + \rho_f\vec{g} - \mu K^{-1}\cdot\vec{q}. \tag{2.2}$$

$$\varepsilon(\rho_0 c)_f\frac{\partial T_f}{\partial t} + (\rho_0 c)_f(\vec{q}\cdot\nabla)T_f = \varepsilon\nabla\cdot(\mathcal{K}\cdot\nabla T_f) + h(T_s - T_f), \tag{2.3}$$

$$(1-\varepsilon)(\rho_0 c)_s\frac{\partial T_s}{\partial t} = (1-\varepsilon)\nabla\cdot(\mathcal{M}\cdot\nabla T_s) - h(T_s - T_f), \tag{2.4}$$

$$\rho_f = \rho_0\{1 - \beta(T_f - T_l)\}. \tag{2.5}$$

Here, $\vec{q} = (u, v, w)$ the velocity vector, T_f the temperature of the fluid, T_s the temperature of the solid, p the pressure, ρ_f the fluid density, μ the fluid viscosity, $\vec{g}$ the gravitational acceleration, ε the porosity of the medium, c the specific heat, β the coefficient of thermal expansion, ρ_0 the reference density and h is the inter-phase heat transfer coefficient, $K = K_h(\hat{i}\hat{i} + \hat{j}\hat{j}) + K_v\hat{k}\hat{k}$ the permeability tensor, $\mathcal{K} = k_{fh}(\hat{i}\hat{i} + \hat{j}\hat{j}) + k_{fv}\hat{k}\hat{k}$ the thermal conductivity tensor of fluid phase and $\mathcal{M} = k_{sh}(\hat{i}\hat{i} + \hat{j}\hat{j}) + k_{sv}\hat{k}\hat{k}$ the thermal conductivity tensor of solid phase, where K_h is the permeability, k_{fh} and k_{sh} are respectively, the thermal conductivity of fluid and solid phases in the horizontal $\hat{i}$ and $\hat{j}$ directions, while K_v, k_{fv} and k_{sv} are the corresponding values in the vertical $\hat{k}$ direction. The time derivative term is taken into consideration in Eq. (2.2) in order to allow the possibility of oscillatory convection as substantiated by Vadasz [17].

The basic state is assumed to be quiescent and is given by

$$\vec{q}_b = 0, \quad p = p_b(z), \quad h = 0, \quad T_{fb} = T_{sb} = -\frac{\Delta T}{d} z + T_l, \tag{2.6}$$

where $\Delta T = T_l - T_u$ and the pressure is of no consequence as we are going to eliminate the same. Now, we consider the stability of the system. To this end, we superimpose infinitesimal disturbances on the basic state as follows:

$$\vec{q} = \vec{q}', \quad p = p_b(z) + p', \quad T_f = T_{fb}(z) + T_f', \quad T_s = T_{sb}(z) + T_s', \tag{2.7}$$

where the prime indicates that the quantities are infinitesimal perturbations. Substituting Eq. (2.7) into Eqs. (2.1)–(2.5), introducing the stream function ψ through $u' = \partial\psi/\partial z, w' = -\partial\psi/\partial x$ and non-dimensionalizing the variables by scaling x, y and z by d, t by $(\rho_0 c)_f d^2/k_{fv}$, ψ by $\varepsilon k_{fv}/(\rho_0 c)_f$, T_f' and T_s' by ΔT, we obtain the following dimensionless equations (after dropping the primes)

$$\left(\frac{\partial}{\partial\tau}\nabla^2 + \frac{\partial^2}{\partial x^2} + \frac{1}{\xi}\frac{\partial^2}{\partial z^2}\right)\psi - \sqrt{Ta}\frac{\partial v}{\partial z} + R\frac{\partial T_f}{\partial x} = 0, \tag{2.8}$$

$$\left(\frac{\partial}{\partial\tau} + \frac{1}{\xi}\right) v + \sqrt{Ta}\frac{\partial\psi}{\partial z} = 0, \tag{2.9}$$

$$\left(\chi\frac{\partial}{\partial\tau} - \frac{\partial^2}{\partial z^2} - \eta_f\nabla_1^2\right)T_f - H(T_s - T_f) = \frac{\partial\psi}{\partial x} + J(\psi, T_f), \tag{2.10}$$

$$\left(\chi\alpha\frac{\partial}{\partial\tau} - \frac{\partial^2}{\partial z^2} - \eta_s\nabla_1^2\right)T_s + \gamma H(T_s - T_f) = 0. \tag{2.11}$$

In the above equations, $R = \beta g K_v \Delta T d/\varepsilon\nu\kappa_{fv}$ is the Darcy-Rayleigh number, $\tau = \chi t$ is the rescaled time, $\chi = Pr\varepsilon/Da$ is the Darcy–Prandtl number or the Vadasz number, $Da = K_v/d^2$ is the Darcy number, $Pr = \nu(\rho_0 c)_f/k_{fv}$ is the effective Prandtl number, $Ta = (2\Omega K_v/\nu\varepsilon)^2$ is the Darcy–Taylor number, $H = hd^2/\varepsilon k_{fv}$ is the inter-phase heat transfer coefficient, $\xi = K_h/K_v$ is the mechanical anisotropy parameter, $\eta_f = k_{fh}/k_{fv}$ is the fluid phase thermal anisotropy parameter, $\eta_s = k_{sh}/k_{sv}$ is the solid phase thermal anisotropy parameter, $\gamma = \varepsilon k_{fv}/(1-\varepsilon)k_{sv}$ is the porosity modified conductivity ratio and $\alpha = k_{fv}/k_{sv}$ is the ratio of conductivities.

The boundaries are impermeable and assumed that the solid and fluid phases have equal temperatures at the bounding surfaces. Hence, the appropriate boundary conditions are:

$$\psi = \frac{\partial v}{\partial z} = T_f = T_s = 0 \quad \text{at} \quad z = 0, 1. \tag{2.12}$$

It is seen that Eqs. (2.8)–(2.11) admit the solution

$$\begin{aligned}
\psi &= A(\tau)\sin(ax)\sin(\pi z),\\
T_f &= B(\tau)\cos(ax)\sin(\pi z) + C(\tau)\sin(2\pi z),\\
T_s &= D(\tau)\cos(ax)\sin(\pi z) + E(\tau)\sin(2\pi z),\\
v &= F(\tau)\sin(ax)\cos(\pi z) + G(\tau)\sin(2\pi x),
\end{aligned} \tag{2.13a-d}$$

where the amplitudes A, B, C, D, E, F and G are functions of time and are to be determined from the dynamics of the system. Substituting Eqs. (2.13a-d) into Eqs. (2.8)–(2.11) and neglecting all higher harmonics generated by their interactions, we obtain the following nonlinear autonomous system of ordinary differential equations:

$$\begin{aligned}
\frac{dA}{d\tau} &= \frac{1}{\delta_1^2}\left[-\left(\frac{1}{\xi}\pi^2 + a^2\right)A - aRB + \pi TaF\right],\\
\frac{dB}{d\tau} &= \frac{1}{\chi}[-aA - \delta_2^2 B + HD - \pi aAC],\\
\frac{dC}{d\tau} &= \frac{1}{\chi}\left[-(4\pi^2 + H)C + HE + \frac{\pi a}{2}AB\right],\\
\frac{dD}{d\tau} &= \frac{1}{\chi\alpha}[\gamma HB - \delta_3^2 D],\\
\frac{dE}{d\tau} &= \frac{1}{\chi\alpha}[\gamma HC - (4\pi^2 + \gamma H)E],\\
\frac{dF}{d\tau} &= -\frac{1}{\xi}F - \pi TaA,
\end{aligned} \tag{2.14a-f}$$

where $\delta_1^2 = \pi^2 + a^2$, $\delta_2^2 = \pi^2 + \eta_f a^2 + H$ and $\delta_3^2 = \pi^2 + \eta_s a^2 + \gamma H$. Eq. (2.14) are the basic set that will be studied in this paper. These equations possess two significant properties. First, the divergence of the flow in phase space,

$$\frac{\partial \dot{A}}{\partial A} + \frac{\partial \dot{B}}{\partial B} + \frac{\partial \dot{C}}{\partial C} + \frac{\partial \dot{D}}{\partial D} + \frac{\partial \dot{E}}{\partial E} + \frac{\partial \dot{F}}{\partial F} = -\left[\frac{1}{\delta_1^2}\left(\frac{1}{\xi}\pi^2 + a^2\right) + \frac{\delta_2^2}{\chi} + \frac{(4\pi^2 + H)}{\chi} + \frac{\delta_3^2}{\chi\alpha} + \frac{(4\pi^2 + \gamma H)}{\chi\alpha} + \frac{1}{\xi}\right], \tag{2.15}$$

is always negative and so the solutions are attracted to a set of measure zero in the phase space: this may be a fixed point, a limit cycle or a strange attractor. The dot above a quantity denotes the derivative with respect to time τ. Second, the equations have an important symmetry as they are unchanged under the transformation

$$(A, B, C, D, E, F) \to (-A, -B, C, -D, E, -F). \tag{2.16}$$

3. Linear stability analysis

Since the solution of weakly nonlinear stability analysis depends on the eigenvalues of the linear stability problem, first the results of linear instability are obtained by neglecting the nonlinear terms from Eq. (2.14a-f) and seeking the solution in the form $\exp(\sigma t)$, where σ is the growth rate. The process finally yields the following dispersion relation:

$$\left[\left(\sigma + \frac{1}{\xi}\right)\left\{\sigma\delta_1^2 + \left(\frac{\pi^2}{\xi} + a^2\right)\right\} + \pi^2 Ta\right]\left\{(\chi\sigma + \delta_2^2)(\chi\alpha\sigma + \delta_3^2) - \gamma H^2\right\} - Ra^2\left(\sigma + \frac{1}{\xi}\right)(\chi\alpha\sigma + \delta_3^2) = 0. \tag{3.1}$$

One of the ways in which Eq. (3.1) may be used to examine the stability of the system will now be discussed. The parameters Ta, H, ξ, η_f, η_s, α, χ, γ and a are taken as given but the Rayleigh number R is considered to be a free parameter and write Eq. (3.1) as

$$R = \frac{1}{a^2\left(\sigma + \frac{1}{\xi}\right)}\left[\left\{\sigma\delta^2 + \frac{\pi^2}{\xi} + a^2\right\}\left(\sigma + \frac{1}{\xi}\right) + \pi^2 Ta\right]\left\{(\chi\sigma + \delta_2^2) - \frac{\gamma H^2}{(\chi\alpha\sigma + \delta_3^2)}\right\}. \tag{3.2}$$

Now we set the real part of σ equal to zero and let $\sigma = i\omega$ in the above equation. After clearing the complex quantities from the denominator, Eq. (3.2) yields

$$R = \frac{1}{a^2\xi(1 + \xi^2\omega^2)(\delta_3^4 + \alpha^2\chi^2\omega^2)}(\Delta_1 + i\omega\Delta_2), \tag{3.3}$$

where

$$\begin{aligned}\Delta_1 = {} & (\delta_3^4 + \alpha^2\chi^2\omega^2)\{\xi(1 + \xi^2\omega^2)(a^2\delta_2^2 - \delta_1^2\chi\omega^2) + \pi^2 Ta\xi^3\chi\omega^2 + \pi^2\delta_2^2(1 + Ta\xi^2 + \xi^2\omega^2)\} \\ & - H^2\gamma\{\xi(1 + \xi^2\omega^2)(a^2\delta_3^2 + \alpha\delta_1^2\chi\omega^2) - \pi^2 Ta\alpha\xi^3\chi\omega^2 + \pi^2\delta_3^2(1 + Ta\xi^2 + \xi^2\omega^2)\},\end{aligned}$$

$$\begin{aligned}\Delta_2 = {} & (\delta_3^4 + \alpha^2\chi^2\omega^2)\{\delta_1^2\delta_2^2\xi(1 + \xi^2\omega^2)(\delta_1^2\delta_2^2 + a^2\chi) + (\pi^2\chi + \pi^2 Ta\xi^2(-\delta_2^2\xi + \chi) + \pi^2\xi^2\chi\omega^2)\} \\ & + H^2\gamma\{(1 + \xi^2\omega^2)(a^2\alpha\chi - \delta_1^2\delta_3^2\xi) + \pi^2 Ta\xi^2(\delta_3^2\xi + \alpha\chi) + \pi^2\alpha\chi(1 + \xi^2\omega^2)\}.\end{aligned}$$

Since R is a physical quantity, it must be real and from Eq. (3.3) it implies either $\omega = 0$ or $\Delta_2 = 0$. Accordingly, we obtain the condition for the occurrence of stationary and oscillatory convection.

The stationary convection (direct bifurcation) corresponds to $\omega = 0$ and it occurs at

$$R^s = \frac{[\pi^2(1 + \xi^2 Ta) + \xi a^2]}{\xi a^2}\frac{\left[(\pi^2 + \eta_f a^2)(\pi^2 + \eta_s a^2) + H\left\{\gamma(\pi^2 + \eta_f a^2) + (\pi^2 + \eta_s a^2)\right\}\right]}{(\pi^2 + \eta_s a^2 + \gamma H)}. \tag{3.4}$$

For the isotropic case ($\xi = \eta_f = \eta_s = 1$), the above expression for R^s reduces to

$$R^s = \frac{\delta^2(\delta^2 + \pi^2 Ta)\{\delta^2 + H(1 + \gamma)\}}{a^2(\delta^2 + \gamma H)}, \tag{3.5}$$

which coincides with the expression obtained by Straughan [19]. When $H \to \infty$ (LTE case), Eq. (3.5) gives the classical result obtained by Palm and Tyvand [26] for the problem of thermal instability in a rotating porous layer. That is,

$$R^s\frac{\gamma}{(1 + \gamma)} = \frac{\delta^2(\delta^2 + \pi^2 Ta)}{a^2}. \tag{3.6}$$

If we set $Ta = 0 = H$ in Eq. (3.4), we obtain

$$R^s = \frac{(\pi^2 + \xi a^2)(\pi^2 + \eta_f a^2)}{\xi a^2}, \tag{3.7}$$

Table 1
Comparison of the asymptotic (A) and exact (E) values of the critical Darcy–Rayleigh number (R_c^s) and the critical wave number (a_c) for different values of H with $Ta = 10$ $\gamma = 0.5$, $\xi = 0.5$, $\eta_f = 5$ and $\eta_s = 5$.

$\log_{10}H$	$R_c^s(A)$	$a_c(A)$	$R_c^s(E)$	$a_c(E)$
−2.0	472.154	3.4182	472.154	3.4182
−1.0	472.774	3.4259	472.774	3.4259
0.0	478.811	3.4993	478.812	3.4996
1.0	528.822	3.8272	528.295	4.0147
3.0	1293.11	4.0687	1287.96	4.0792
4.0	1403.37	3.4722	1403.37	3.4722
5.0	1414.96	3.4227	1414.96	3.4227

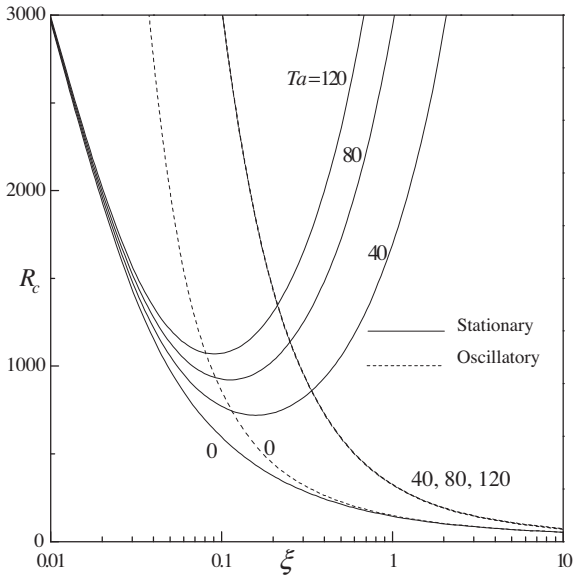

Fig. 1. Variation of R_c as a function of ξ for different values of Ta when $\eta_f = 2$ and $\eta_s = 2$.

Ta	$(R_c)_{\min}$	$(\xi_c)_{\min}$
20	493.142	0.224
40	622.417	0.158
80	750.281	0.112
120	828.832	0.112

The values of $(R_c)_{\min}$ and $(\xi_c)_{\min}$ for various vales of Ta are also given.

and this coincides with Epherre [27]. The asymptotic analyses for small and large values of H are carried out as outlined in and the results are compared with those obtained from the exact formula given by Eq. (3.4) in Table 1 and good agreement is found.

The oscillatory onset (Hopf bifurcation) corresponds to $\Delta_2 = 0\,(\omega \neq 0)$ in Eq. (3.3) and this gives a dispersion relation of the form

$$c_1(\omega^2)^2 + c_2(\omega^2) + c_3 = 0, \tag{3.8}$$

where

$$c_1 = \alpha^2\xi^2\chi^2\,(\delta_1^2\delta_2^2\xi + \chi\pi^2 + \chi a^2\xi),$$

$$c_2 = H^2\gamma\xi^2(\alpha\pi^2\chi + a^2\xi\chi - \delta_1^2\delta_3^2\xi) + \delta_1^2\delta_2^2\xi^3\delta_3^4 + \delta_1^2\delta_2^2\xi\alpha^2\chi^2 + \chi a^2\xi^3\delta_3^4 + \chi^3 a^2\xi\alpha^2 + \pi^2\chi^2\delta_3^4\xi^2 + \alpha^2\chi^2(\chi + Ta\xi^2\chi - \delta_2^2 Ta\xi^3),$$

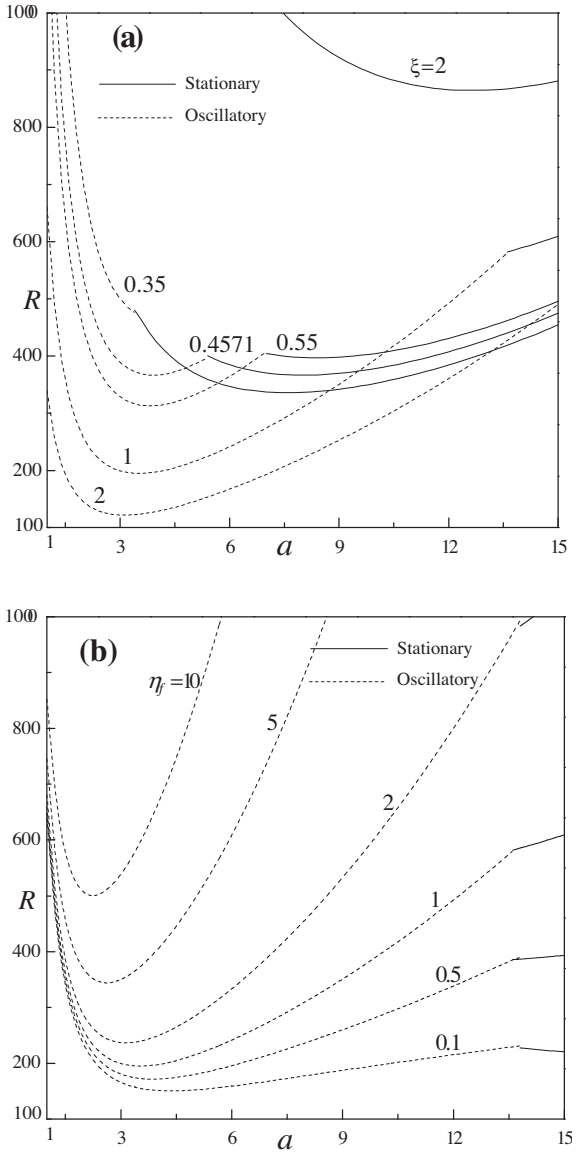

Fig. 2. Neutral curves for different values of (a) ξ with $\eta_f = 1$ and (b) η_f with $\xi = 1$ when $\gamma = 0.5$, $Ta = 20$, $\eta_s = 1$, $\alpha = 0.01$, $H = 100$ and $\chi = 1$.

$$c_3 = \delta_3^4\{\delta_1^2\delta_2^2\xi + a^2\xi\chi + \pi^2\chi + \pi^2 Ta\xi^2(\chi - \delta_2^2\xi)\} + H^2\gamma\{a^2\alpha\xi\chi - \delta_1^2\delta_3^2\xi + \pi^2\alpha\chi + \pi^2 Ta\xi^2(\alpha\chi + \delta_3^2\xi)\}.$$

When $\Delta_2 = 0\,(\omega \neq 0)$, Eq. (3.3) gives the condition for the occurrence of oscillatory convection and it occurs at $R = R^o$, where

$$R^o = \frac{\left[(\delta_3^4 + \alpha^2\chi^2\omega^2)\{\xi(1+\xi^2\omega^2)(a^2\delta_2^2 - \delta_1^2\chi\omega^2) + \pi^2 Ta\xi^3\chi\omega^2 + \pi^2\delta_2^2(1 + Ta\xi^2 + \xi^2\omega^2)\} - H^2\gamma\{\xi(1+\xi^2\omega^2)(a^2\delta_3^2 + \alpha\delta_1^2\chi\omega^2) - \pi^2 Ta\alpha\xi^3\chi\omega^2 + \pi^2\delta_3^2(1 + Ta\xi^2 + \xi^2\omega^2)\}\right]}{a^2\xi(1+\xi^2\omega^2)(\delta_3^4 + \alpha^2\chi^2\omega^2)}. \tag{3.9}$$

The critical value of R^o with respect to the wave number is determined as follows. For fixed parametric values, Eq. (3.8) is solved first to determine the positive values of ω^2. If there are none, then no Hopf bifurcation is possible. If there is only one positive value of ω^2 then the critical value of R^o with respect to wave number is computed numerically from Eq. (3.9). If there are two positive values of ω^2, then the minimum of R^o amongst these two ω^2 is retained to find the critical value of R^o with respect to the wave number.

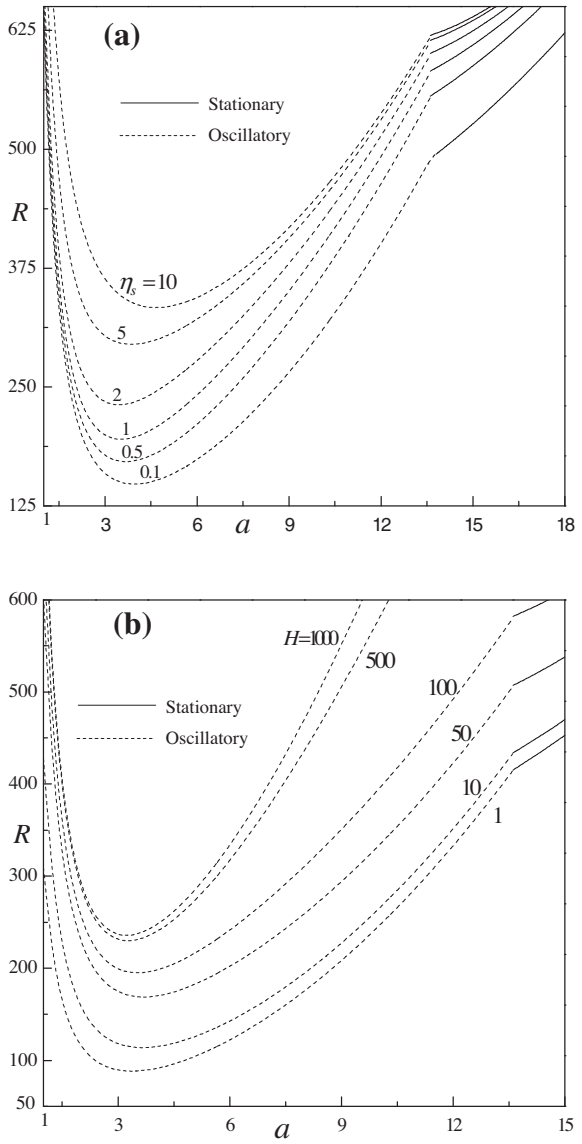

Fig. 3. Neutral curves for different values of (a) η_s with $H = 100$ and (b) H with $\eta_s = 1$ when $\gamma = 0.5$, $Ta = 20$, $\xi = 1$, $\eta_f = 1$, $\alpha = 0.01$ and $\chi = 1$.

4. Weakly nonlinear stability analysis

The nonlinear system of autonomous differential equations (2.14a-f) is not amenable to analytical treatment, in general. Nonetheless, for the steady case the solution can be obtained at once. Such solutions are useful because they predict that a finite amplitude solution to the system is possible for subcritical values of the Rayleigh number or not and that the minimum values of R for which a steady solution is possible lies below the critical values of R^s or R^o. Setting the left-hand sides of Eqs. (2.14a-f) equal to zero and eliminating the amplitude F, we obtain

$$\{a^2\xi + \pi^2(1 + \xi^2 Ta)\}A + aR\xi B = 0,$$
$$aA + \delta_2^2 B - HD + \pi aAC = 0,$$
$$2(4\pi^2 + H)C - 2HE - \pi aAB = 0,$$
$$\gamma HB - \delta_3^2 D = 0,$$
$$\gamma HC - (4\pi^2 + \gamma H)E = 0. \qquad (4.1a\text{-}e)$$

The steady state solutions are useful because they predict that a finite amplitude solution to the system is possible for sub-critical values of a Rayleigh number and that the minimum values of finite amplitude Rayleigh number lies below the critical for instability to either a marginal state or an overstable infinitesimal perturbation.

Expressing the amplitudes B, C, D and E in terms A using Eq. (4.1a-e), we obtain

$$B = -\frac{a\delta_3^2(4\pi^2 + H\gamma + H)A}{\left(\delta_2^2\delta_3^2 - \gamma H^2\right)(4\pi^2 + H\gamma + H) + a^2\delta_3^2(4\pi^2 + \gamma H)(A^2/8)},$$

$$C = -\frac{1}{\pi}\left[\frac{a^2\delta_3^2(4\pi^2 + H\gamma)(A^2/8)}{\left(\delta_2^2\delta_3^2 - \gamma H^2\right)(4\pi^2 + H\gamma + H) + \delta_3^2a^2(4\pi^2 + \gamma H)(A^2/8)}\right],$$

$$D = \frac{-a\gamma H(4\pi^2 + H\gamma + H)A}{\left(\delta_2^2\delta_3^2 - \gamma H^2\right)(4\pi^2 + H\gamma + H) + \delta_3^2a^2(4\pi^2 + \gamma H)(A^2/8)},$$

$$E = \frac{-a^2\gamma H\delta_3^2(A^2/8)}{\left(\delta_2^2\delta_3^2 - \gamma H^2\right)(4\pi^2 + H\gamma + H) + a^2\delta_3^2(4\pi^2 + \gamma H)(A^2/8)}. \quad (4.2a\text{-}d)$$

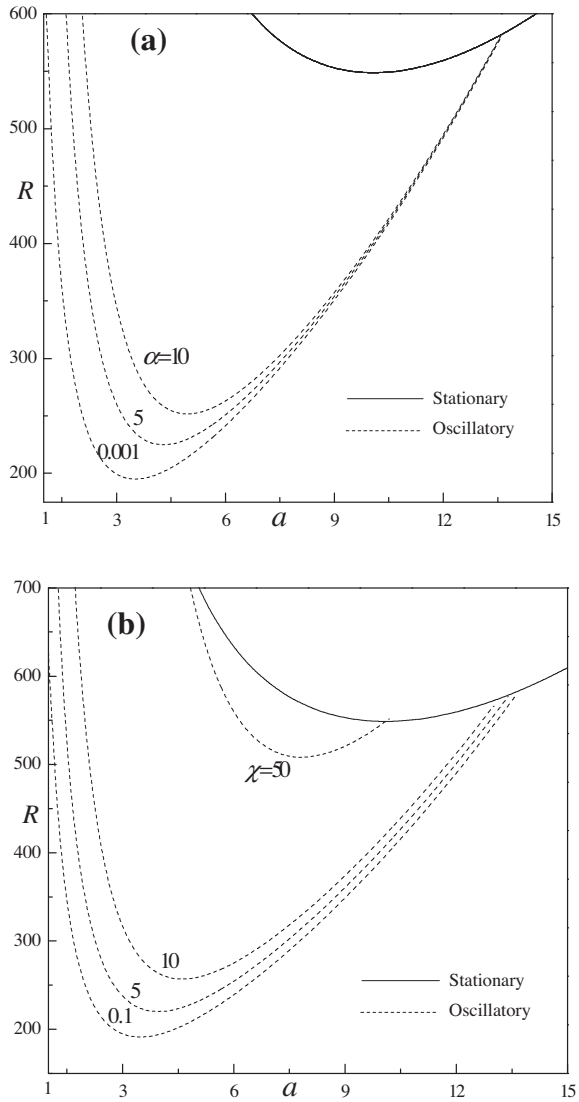

Fig. 4. Neutral curves for different values of (a) α with $\chi = 1$ and (b) χ with $\alpha = 0.01$ when $\gamma = 0.5$, $Ta = 20$, $\xi = 1$, $\eta_f = 1$, $\eta_s = 1$ and $H = 100$.

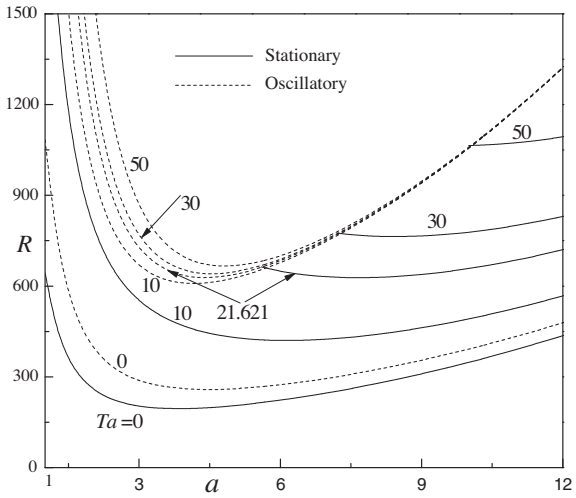

Fig. 5. Neutral curves for different values of Ta when $\alpha = 0.01$, $\gamma = 0.5$, $\chi = 10$, $\xi = 0.5$, $\eta_f = 2$, $\eta_s = 2$ and $H = 100$.

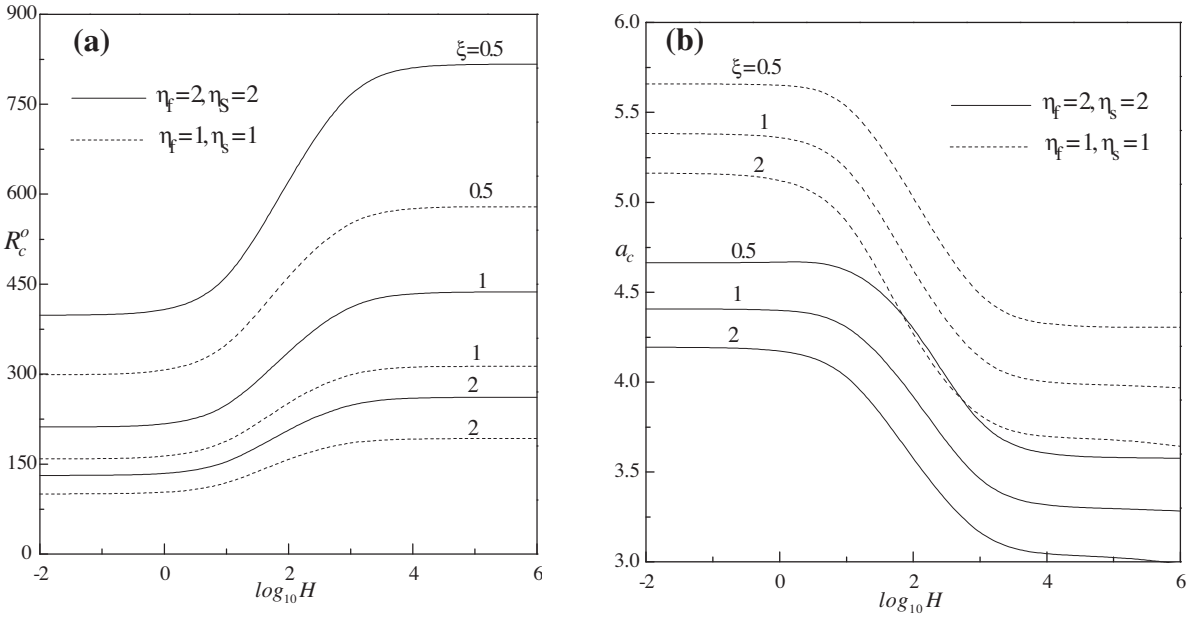

Fig. 6. Variation of (a) R_c^o and (b) a_c with $log_{10}H$ for different values of ξ with $Ta = 20$, $\gamma = 0.5$, $\alpha = 0.01$ and $\chi = 10$.

We now obtain from Eq. (4.1a)

$$A\left\{a^2\xi + \pi^2(1+\xi^2 Ta) - a^2 R\xi\left[\frac{\left(\delta_2^2\delta_3^2 - \gamma H^2\right)}{\delta_3^2} + \frac{a^2(4\pi^2+\gamma H)}{(4\pi^2+H\gamma+H)}\left(\frac{A^2}{8}\right)\right]^{-1}\right\} = 0. \tag{4.3}$$

The solution $A = 0$ corresponds to pure conduction, which we know to be a possible solution, though it is unstable when the Rayleigh number R is sufficiently large. The remaining solutions are given by

$$\frac{A^2}{8} = \left[\frac{(4\pi^2+H\gamma+H)}{(4\pi^2+\gamma H)}\right]\left\{\frac{R\xi}{a^2\xi+\pi^2(1+\xi^2 Ta)} - \frac{\left(\delta_2^2\delta_3^2-\gamma H^2\right)}{a^2\delta_3^2}\right\}. \tag{4.4}$$

Further using Eq. (3.4) in the above equation, we obtain

$$\frac{A^2}{8} = \left[\frac{(4\pi^2 + H\gamma + H)\xi}{(4\pi^2 + \gamma H)\{a^2\xi + \pi^2(1 + \xi^2 Ta)\}}\right](R - R^s). \tag{4.5}$$

The expression for the finite amplitude Rayleigh number R^f is thus given by

$$R^f = R^s + \frac{(4\pi^2 + \gamma H)\{a^2\xi + \pi^2(1 + \xi^2 Ta)\}}{\xi(4\pi^2 + H\gamma + H)}\left(\frac{A^2}{8}\right). \tag{4.6}$$

From Eq. (4.6) it is observed that R^f attains its critical value at $a^2 = a_c^2$ and $A = 0$. As a result of this, it is noted that the critical value of R^f for any chosen parametric values turns out to be same as that of steady onset indicating the equivalence of the linear and weakly nonlinear stability boundaries. This observed result is in conformity with the isotropic case discussed by Straughan [5] using global stability analysis.

Using Eq. (4.5) in Eq. (4.2b), we obtain

$$C = -\frac{1}{\pi}\left(1 - \frac{R^s}{R}\right). \tag{4.7}$$

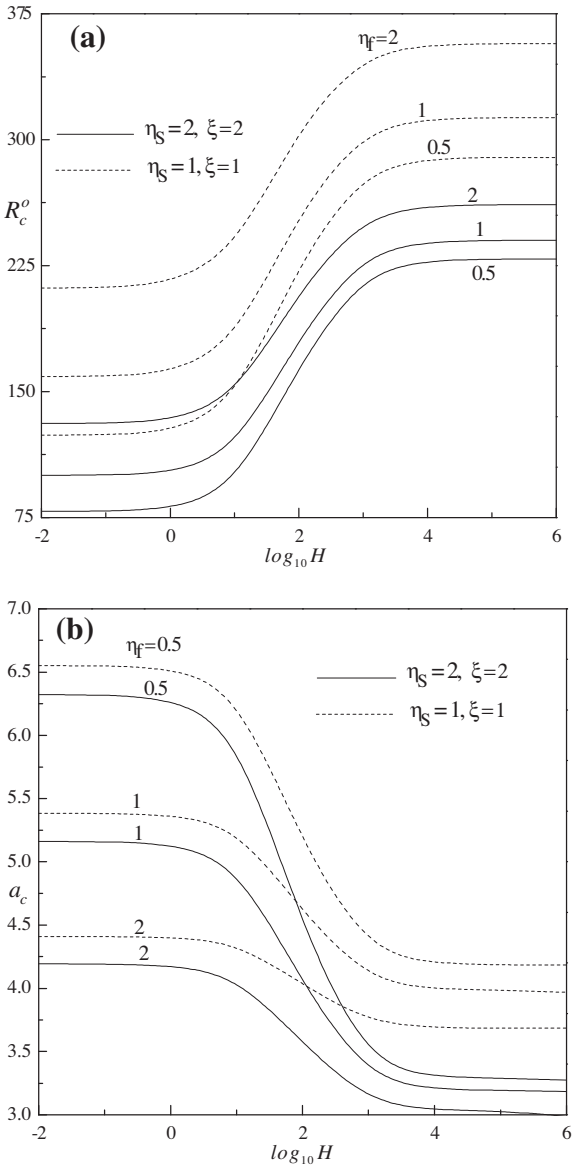

Fig. 7. Variation of (a) R_c^o and (b) a_c with $log_{10}H$ for different values of η_f with $Ta = 20$, $\gamma = 0.5$, $\alpha = 0.01$ and $\chi = 10$.

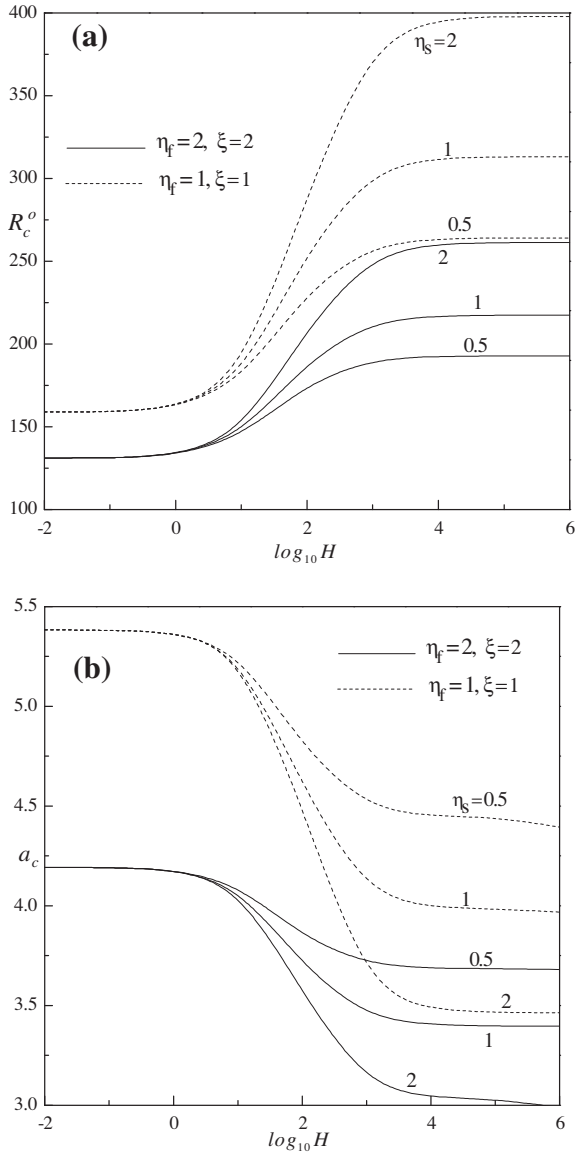

Fig. 8. Variation of (a) R_c^o and (b) a_c with $log_{10}H$ for different values of η_s with $Ta = 20$, $\gamma = 0.5$, $\alpha = 0.01$ and $\chi = 10$.

4.1. Heat transport

In the study of convection, the quantification of heat transport is important. This is because onset of convection, as Rayleigh number is increased, is more readily detected by its effect on the heat transport. If $\bar{H}$ is the rate of heat transport per unit area for the fluid phase, then

$$\bar{H} = -\kappa_f \left\langle \frac{\partial T_{f_{total}}}{\partial z} \right\rangle_{z=0}, \tag{4.8}$$

where the angular brackets correspond to a horizontal average and

$$T_{f_{total}} = T_l - \Delta T \frac{z}{d} + T_f(x, z, t). \tag{4.9}$$

Substituting Eq. (4.1b) into Eq. (4.9) and using the resultant equation in Eq. (4.8), we get

$$\bar{H} = \frac{\kappa_f \Delta T}{d}(1 - 2\pi C). \tag{4.10}$$

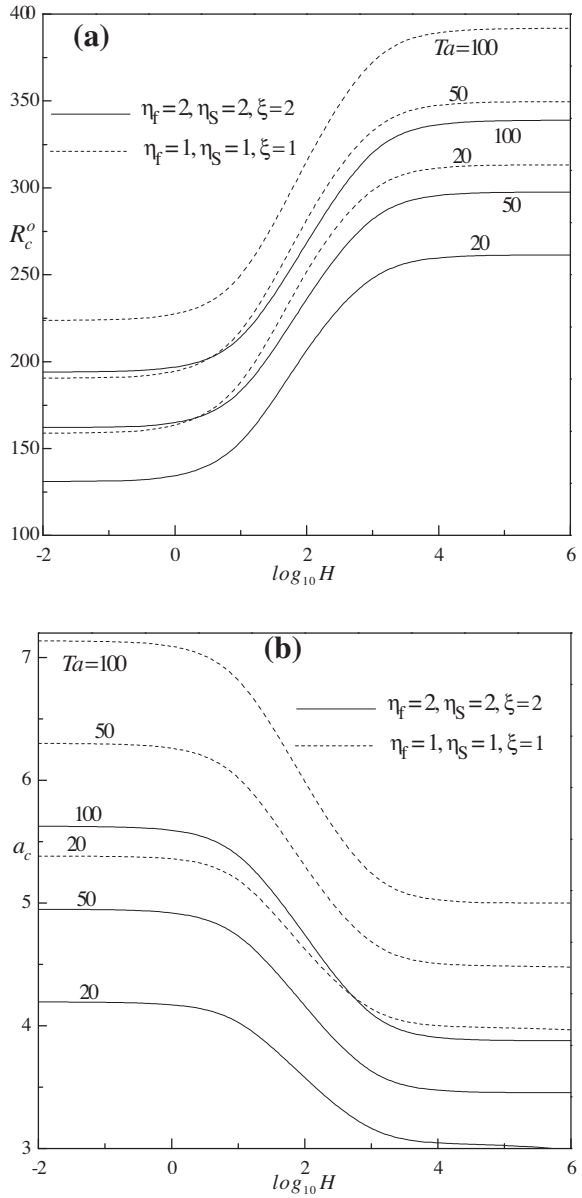

Fig. 9. Variation of (a) R_c^o and (b) a_c with $log_{10}H$ for different values of Ta with $\gamma = 0.5$, $\alpha = 0.01$ and $\chi = 10$.

The Nusselt number Nu for the fluid phase is defined by

$$Nu = \frac{\bar{H}}{\kappa_f \Delta T/d} = 1 - 2\pi C. \tag{4.11}$$

Substituting Eq. (4.7) into Eq. (4.11), one can obtain

$$Nu = 1 + 2\left(1 - \frac{R^s}{R}\right). \tag{4.12}$$

5. Results and discussion

Thermal convective instability in a rotating anisotropic porous layer is investigated using a local thermal non-equilibrium (LTNE) model. A weakly nonlinear stability analysis is carried out by constructing model equations using minimal representation of Fourier series and established the equivalence of the linear and weakly nonlinear stability boundaries indicating the

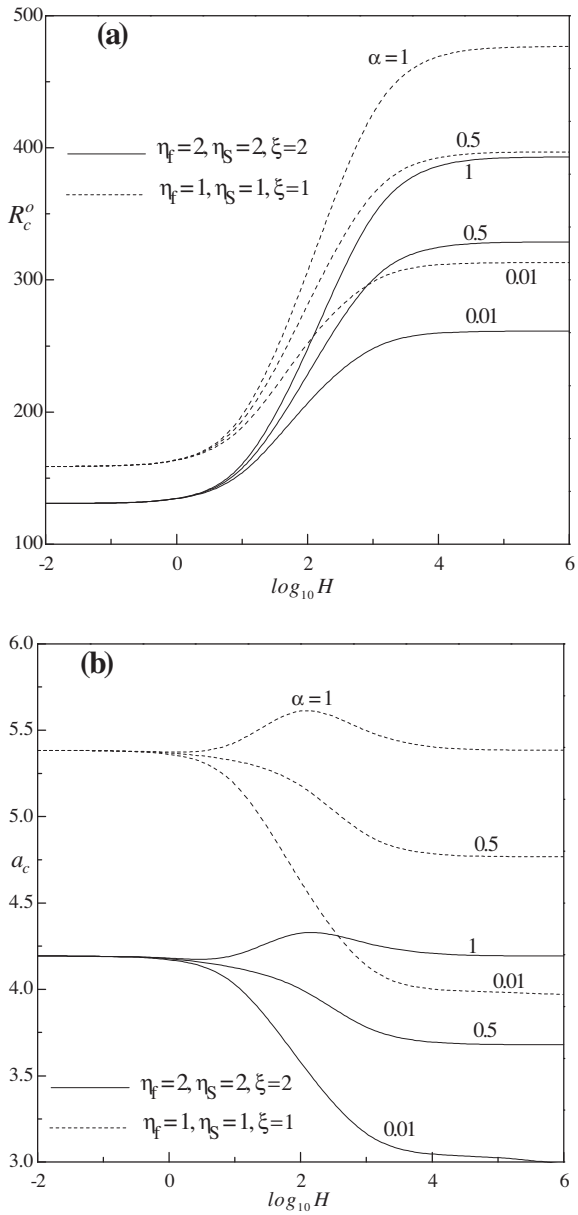

Fig. 10. Variation of (a) R_c^o and (b) a_c with $log_{10}H$ for different values of α with $Ta = 20$, $\gamma = 0.5$ and $\chi = 10$.

linearized instability theory captures completely the physics of the onset of convection. In addition, the heat transport is calculated in terms of Nusselt number and streamlines and isotherms are exhibited for some chosen parametric values.

From Eq. (3.4) it is noted that

$$\frac{\partial R^s}{\partial \xi} = \frac{\pi^2}{a^2}\left(-\frac{1}{\xi^2} + Ta\right)\frac{\left[\left(\pi^2+\eta_f a^2\right)(\pi^2+\eta_s a^2) + H\left\{\gamma(\pi^2+\eta_f a^2) + (\pi^2+\eta_s a^2)\right\}\right]}{(\pi^2+\eta_s a^2+\gamma H)}. \tag{5.1}$$

At $Ta = 0$, it is observed that R^s is a decreasing function of mechanical anisotropy parameter ξ indicating its effect is to hasten the onset of convection. When $Ta \neq 0$, however, it is seen that the right-hand side of Eq. (5.1) may be either negative or positive depending on the value of Ta and ξ. That is to say that an increase in the value of ξ may not be always a destabilizing factor and may stabilize the rotating fluid saturated anisotropic porous layer. In fact R^s attains its minimum with respect to ξ at $\xi = 1/\sqrt{Ta}$, below this value the system becomes unstable and above which the system becomes stable. Thus, in the presence of rotation the mechanical anisotropy parameter plays a dual role on the stability characteristics of the system. This

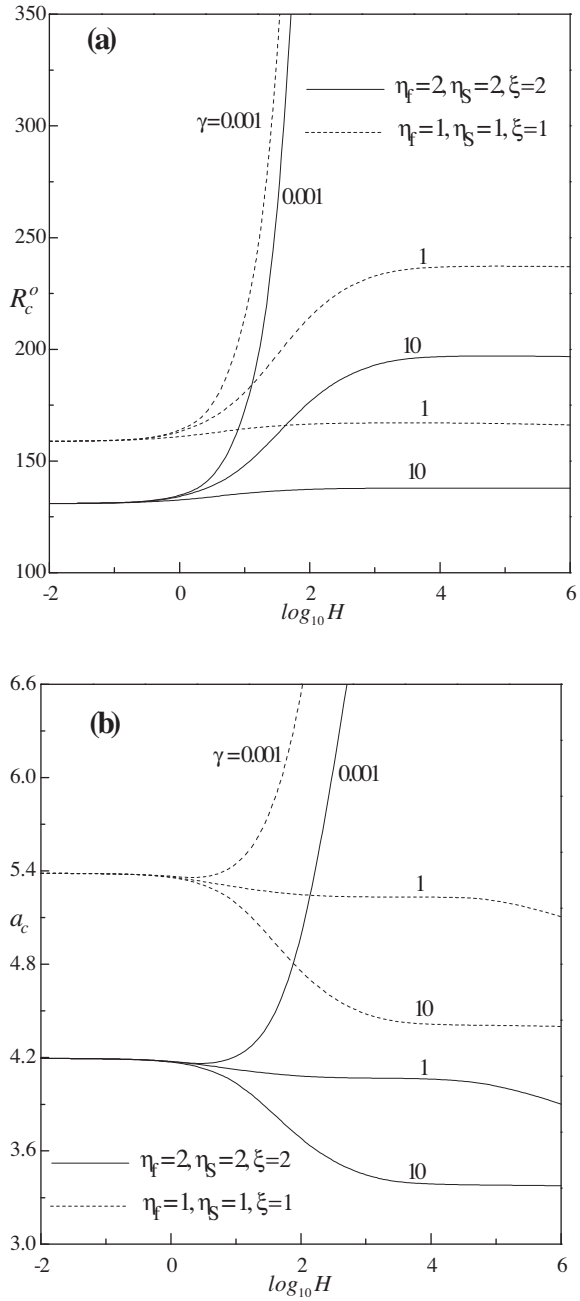

Fig. 11. Variation of (a) R_c^o and (b) a_c with $log_{10}H$ for different values of γ with $Ta = 20$, $\alpha = 0.01$ and $\chi = 10$.

aspect has been elucidated graphically in Fig. 1 and it is seen that the critical Rayleigh number R_c^s, obtained with respect to wave number, passes through a minimum with increasing ξ for values of $Ta \neq 0$. In other words, ξ exhibits both destabilizing and stabilizing effects on the stationary onset in the presence of rotation. To the contrary, it is observed that the critical Rayleigh number R_c^o for the oscillatory case decreases with increasing ξ for all values of Taylor number and thereby showing it has only destabilizing effect on the oscillatory onset. From the figure it is also evident that, for a fixed value of non-zero Taylor number, steady convection is preferred up to certain value of ξ and exceeding which the instability switches over to oscillatory type as the curves of R_c^s and R_c^o intersect.

Figs. 2–5 show the neutral stability curves on the (R, a)-plane. The solid and dashed curves represent the stationary and the oscillatory modes, respectively. Fig. 2a shows the neutral curves for several assigned values of mechanical anisotropy parameter ξ. From the figure it is seen that the influence of ξ on the stability of the system depends on the nature of onset

of convection viz., steady or oscillatory. It is observed that increasing ξ is to increase the steady onset Rayleigh number while opposite is the trend with oscillatory onset Rayleigh number. A closer inspection of the figure further reveals that there exists a threshold value of $\xi(=\xi^*)$ below which the preferred mode of instability is via stationary convection and beyond which the convection sets in as oscillatory motions. For the chosen values of $Ta = 20$, $\eta_s = 1 = \eta_f$, $\alpha = 0.01$, $H = 100$ and $\chi = 1$ it is found that the value of $\xi^* = 0.4571$. Fig. 2b indicates that increasing the fluid phase thermal anisotropy parameter η_f is to increase the region of stability and a similar trend could be seen with increasing solid phase thermal anisotropy parameter η_s (Fig. 3a). The region of stability increases with an increase in the value of interphase heat transfer coefficient H (Fig. 3b). Besides, oscillatory convection is the preferred mode of instability for all the values of η_f, η_s and H considered. The ratio of conductivities α (Fig. 4a) and the Darcy–Prandtl number χ (Fig. 4b) affect only the onset of oscillatory convection and their effect is to increase the region of stability. Moreover, the oscillatory neutral curves for different values of α bifurcate from the stationary neutral curve at the same wave number. Fig. 5 exhibits the neutral curves for different values of Ta when $\alpha = 0.01$,

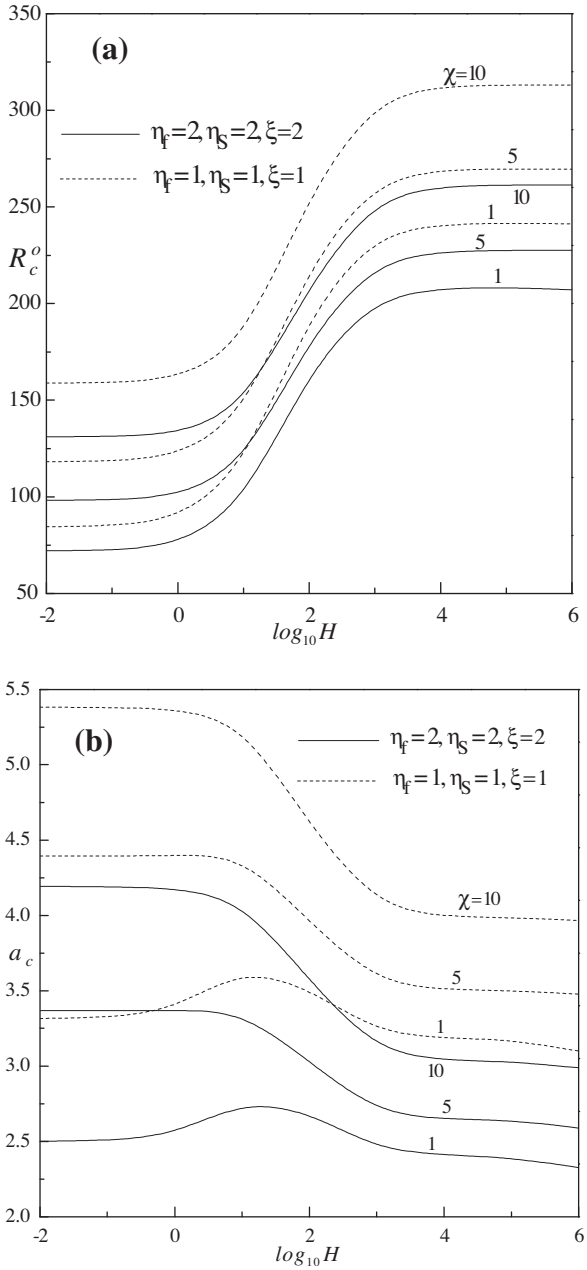

Fig. 12. Variation of (a) R_c^o and (b) a_c with $log_{10}H$ for different values of χ with $Ta = 20$, $\gamma = 0.5$ and $\alpha = 0.01$.

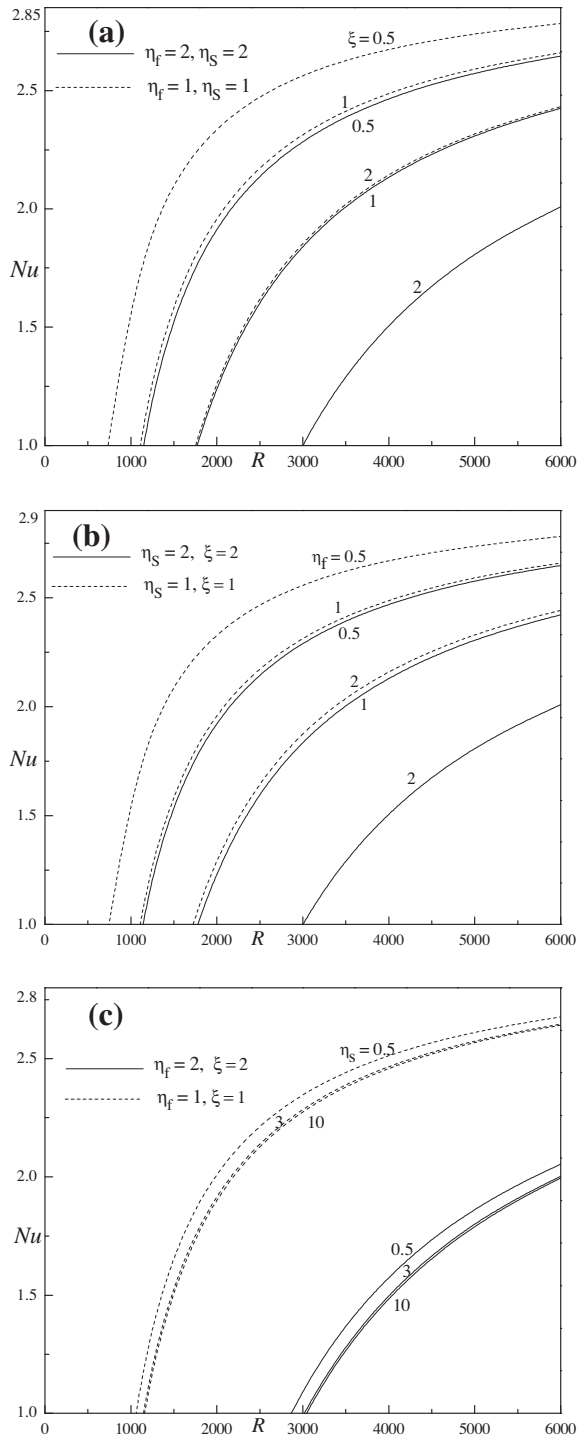

Fig. 13. Variation of *Nu* with *R* for different values of (a) ξ (b) η_f and (c) η_s when $Ta = 50$, $\gamma = 0.5$ and $H = 100$.

$\gamma = 0.5$, $\chi = 10$, $\xi = 0.5$, $\eta_f = 2$, $\eta_s = 2$ and $H = 100$. There exists a threshold value of $Ta(= Ta^*)$ below which stationary and above which oscillatory convections are the preferred mode of instabilities. For the chosen parametric values, it is found that $Ta^* = 21.621$.

The variation of critical stability parameters (R_c^o, a_c) is shown in Figs. 6–12 as a function of $\log_{10}H$ for various values of physical parameters since the oscillatory convection is the preferred mode of instability. The results for $\xi = \eta_f = \eta_s = 1$

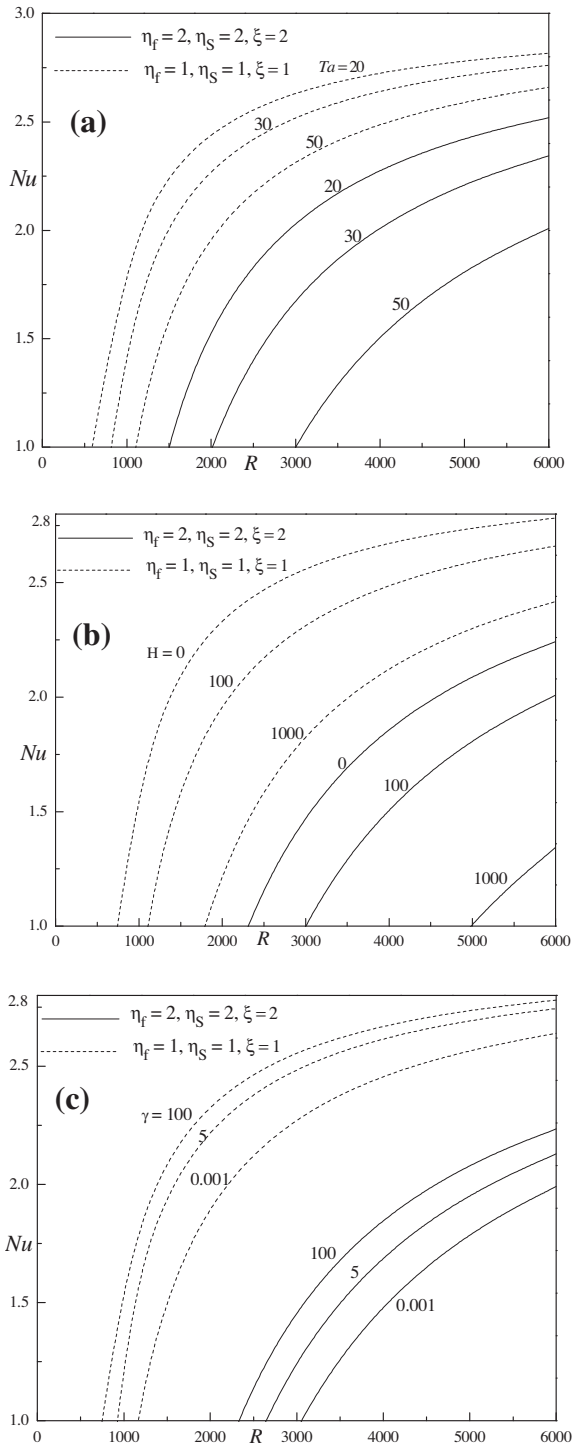

Fig. 14. Variation of *Nu* with *R* for different values of (a) *Ta* with $\gamma = 0.5$, $H = 100$. (b) *H* with $Ta = 50$, $\gamma = 0.5$ and (c) γ with $Ta = 50$, $H = 100$.

correspond to isotropic case. The effect of decreasing mechanical anisotropy parameter ξ is to delay the onset of convection (Fig. 6a) and to increase the critical wave number (Fig. 6b). This is because, decrease in ξ corresponds to smaller horizontal permeability which in turn hinders the motion of the fluid in the horizontal direction. As a consequence, the conduction process in the rotating porous medium becomes more stable and hence higher values of Rayleigh number are needed for the onset of convection. The larger resistance to horizontal flow also leads to a shortening of the horizontal wavelength (i.e., increase in the horizontal wave number) at the onset of convection. To the contrary, decrease in the value of η_f (Fig. 7a)

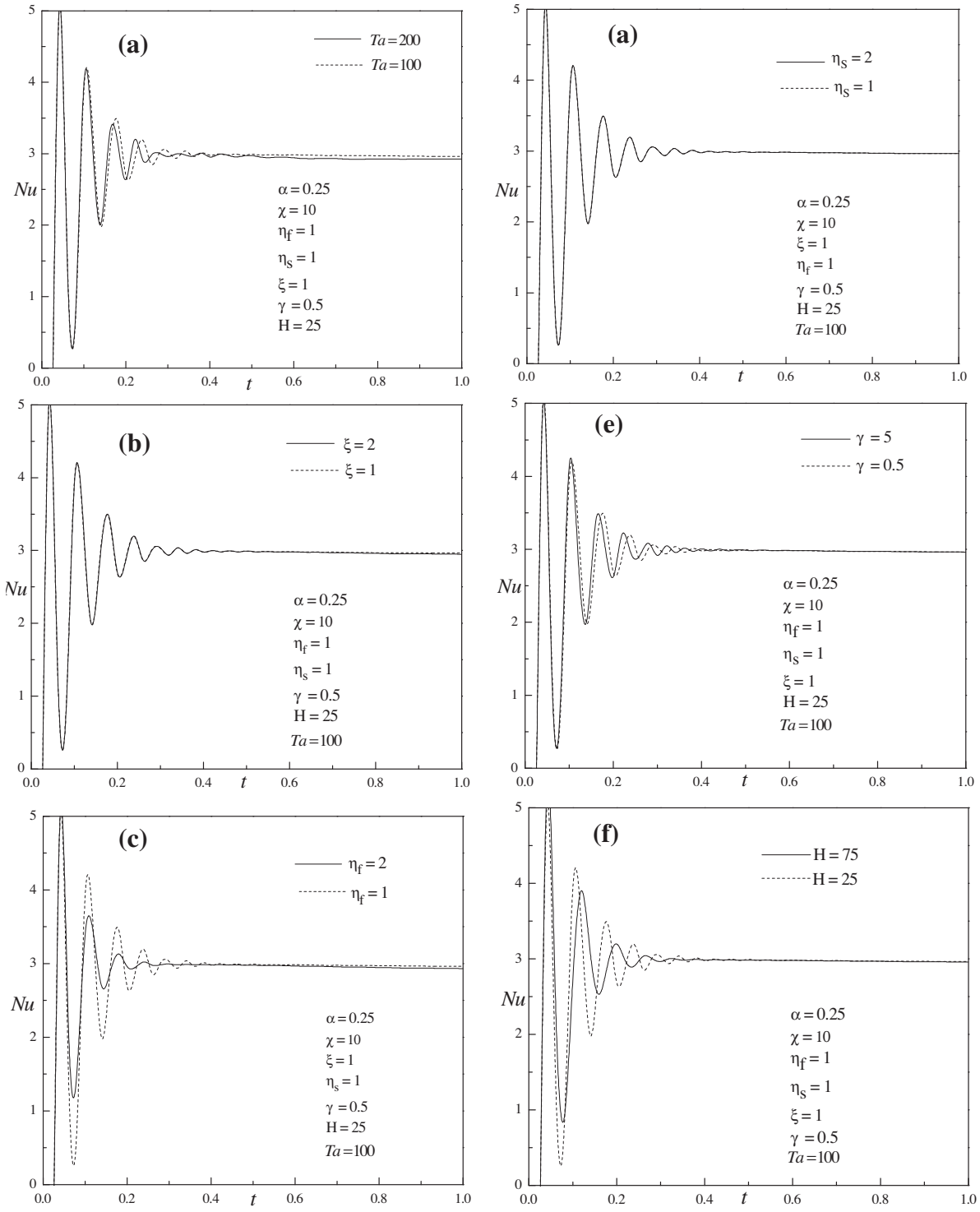

Fig. 15. Variation of Nusselt number with time t for different values of (a) Ta, (b) ξ, (c) η_f, (d) η_s, (e) γ and (f) H when $R = 75,000$.

and η_s (Fig. 8a) hasten the onset of convection. This may be attributed to the fact that, as η_f or η_s decreases the horizontal thermal diffusivity also decreases. Thus heat cannot be transported through the rotating porous layer freely and hence the horizontal temperature variations in the fluid required to sustain convection are less efficiently dissipated for small η_f or η_s. Hence, the base state becomes less stable leading to the onset of convection at lower values of the Rayleigh number. The

critical wave number is found to increase with decreasing η_f (Fig. 7b) and η_s (Fig 8b). From Fig. 8a and b it is further seen that R_c^o and a_c remain unaltered for different values of η_s at smaller values of H (LTE limit).

The effect of rotation is to delay the onset of convection because its effect is to suppress vertical motion and thereby restricts the motion to the horizontal plane (Fig. 9a). It is observed that R_c^o values increase with increasing $\log_{10}H$ but opposite is the case with a_c (Fig. 9b). Moreover, increasing the Taylor number is to increase the critical wave number and hence its effect is to diminish the size of convection cells. The influence of ratio of conductivities α and the porosity modified conductivities ratio γ on the stability characteristics of the system is illustrated respectively in Figs. 10 and 11. From these figures it is noted that the curves of R_c^o and a_c for different values of α and γ coalesce at smaller values of H while they exhibit contrasting behavior on the stability of the system at moderate and higher values of H. It is also observed that the effect of increasing α is to delay the onset of convection (Fig. 10a) and also to increase the critical wave number (Fig. 10b). But the trend noticed with increasing γ is found to be opposite in nature (Fig. 11a and b). The effect of Darcy–Prandtl number χ on R_c^o and a_c is displayed in Fig. 12a and b respectively. The figures reveal that the rotating porous layer gets stabilized as the value of R_c^o increases with increasing χ (Fig. 12a) and also there is an increase in the critical wave number with χ (Fig. 12b).

A general observation that can be made from the results presented in Figs. 6–12 is that the stability characteristics of the system is independent of H when $H << 1$ and $H >> 1$ but found to be significant only at intermediate values of H. This may be attributed to the fact that, when $H \to 0$, there is almost no transfer of heat between the fluid and solid phases and the properties of solid phase have no significant influence on the onset of convection. On the other hand, when $H \to \infty$, the fluid and solid phases have almost equal temperatures and therefore may be treated as a single phase. Between these two extreme cases, H gives rise to a strong non-equilibrium effect and its effect is to make the system more stable. Moreover, the critical stability parameters R_c^o and a_c values for the isotropic case ($\xi = \eta_f = \eta_s = 1$) are higher than those of anisotropic case of $\xi = \eta_f = \eta_s = 2$.

The vigor of convection is measured by the heat transfer across the porous layer and is calculated in terms of Nusselt number Nu. The variation of Nusselt number with Rayleigh number is shown in Figs. 13a–c and 14a–c for different values of physical parameters and it is seen that the Nusselt number increases with the increase in the value of Rayleigh number. Fig. 13a–c respectively show the variation of triplets (ξ, η_f, η_s) on the Nusselt number. For the parametric values chosen, increasing ξ, η_f and η_s is to decrease the Nusselt number and hence their effect is to reduce the heat transfer across the porous layer. Further, the effect of η_s on the heat transfer is found to be not so significant compared to other two anisotropic parameters. The effect of increasing the Taylor number and interphase heat transfer coefficient is to lower the values of Nusselt number reiterating their stabilizing influence on the system while increasing γ shows an opposite behavior on the heat transfer. These facts are evident from the variation of triplets (Ta, H, γ) exhibited on Nu in Fig. 14a–c respectively. The values of Nu for the isotropic case $\xi = 1 = \eta_f = \eta_s$ are higher correspond to the anisotropic case of $\xi = 2 = \eta_f = \eta_s$.

The nonlinear autonomous system of differential equations given by Eq. (2.20a-f) is solved numerically with appropriate initial conditions and the transient behavior of the Nusselt number is displayed in Fig. 15a–f for selected values of physical parameters. It is observed that there is an excellent agreement between the steady state values of Nu obtained analytically and the transient Nu computed numerically for large time t.

6. Conclusions

Thermal convective instability in a horizontal fluid-saturated anisotropic porous layer rotating about a vertical axis is investigated when the fluid and solid phases of the porous medium are in local thermal non-equilibrium (LTNE). It is found that, depending on the parametric values, there exists a threshold value of mechanical anisotropy parameter as well as Taylor number below which the preferred mode of instability occurs via stationary convection and beyond which the convection sets in as oscillatory convection. The system behaves like a LTE model at large and small values of interphase heat transfer coefficient, while the intermediate values show strong influence on both stationary and oscillatory modes. The rotation has stabilizing effect on both stationary and oscillatory convection. Although the effect of increasing mechanical anisotropy parameter is to hasten the onset of steady convection in the absence of rotation, it shows both stabilizing and destabilizing effects in the presence of rotation. Nonetheless, the onset of oscillatory convection in the presence of rotation is advanced with increasing mechanical anisotropy parameter. The effect of increasing thermal anisotropy parameters is to delay the onset of both steady and oscillatory convection. Since there is no transfer of heat between the solid and fluid phases at small values of interphase heat transfer coefficient, the ratio of conductivities and porosity modified conductivity ratio found to have no influence on the onset criterion. At higher values of interphase heat transfer coefficient, however, their effect is to delay and hasten the onset of oscillatory convection, respectively. Besides, the effect of Vadasz number is to delay the onset of oscillatory convection. The weakly nonlinear stability analysis carried out reveals the equivalence of linear and weakly nonlinear stability boundaries. Increase in the values of thermal anisotropy parameters is to decrease the Nusselt number and hence their effect is to reduce the heat transfer across the porous layer. The rotation and the interphase heat transfer coefficient have a retarding effect on heat transfer, while the porosity modified conductivity ratio has enhancing effect. The heat transfer for the isotropic case is higher compared to the anisotropic case. The transient Nusselt number computed compare well with the results of steady state Nusselt number at large time t.

Acknowledgment

The authors (A.L.M) and (M.R) wish to thank their respective Principals of their colleges for encouragement.

References

[1] L. Virto, M. Carbonell, R. Castilla, P.J. Gamez-Montero, Heating of saturated porous media in practice: several causes of local thermal non-equilibrium, Int. J. Heat Mass Transfer 52 (2009) 5412–5422, http://dx.doi.org/10.1016/j.ijheatmasstransfer.2009.07.003.
[2] B. Straughan, Porous convection with local thermal non-equilibrium temperatures and with Cattaneo effects in the solid, Proc. R. Soc. A 469 (2013) 20130187.
[3] N. Banu, D.A.S. Rees, Onset of Darcy–Bénard convection using a thermal non-equilibrium model, Int. J. Heat Mass Transfer 45 (2002) 2221–2228, http://dx.doi.org/10.1016/S0017-9310(01)00331-3.
[4] M.S. Malashetty, I.S. Shivakumara, K. Sridhar, The onset of Lapwood–Brinkman convection using a thermal non-equilibrium model, Int. J. Heat Mass Transfer 48 (2005) 1155–1163.
[5] B. Straughan, Global non-linear stability in porous convection with a thermal non-equilibrium model, Proc. R. Soc. London 462 (2006) 409–418.
[6] K. Vafai (Ed.), Handbook of Porous Media, edited, Marcel Dekker, New York, 2000.
[7] K. Vafai (Ed.), Handbook of Porous Media, Taylor and Francis/CRC, Boca Raton, FL, 2005.
[8] P. Vadasz (Ed.), Emerging Topics in Heat and Mass Transfer in Porous Media, Springer, New York, 2008.
[9] D.A. Nield, A. Bejan, Convection in Porous Media, 4th ed., Springer-Verlag, New York, 2013.
[10] R. McKibbin, Thermal convection in layered and anisotropic porous media: a review, in: R.A. Wooding, I. White (Eds.) Convective Flows in Porous Media, Department of Scientific and Industrial Research, Wellington, 1985, pp. 113–127.
[11] R. McKibbin, Convection and heat transfer in layered and anisotropic porous media, in: M. Quintard, M. Todorovic (Eds.), Heat and Mass Transfer in Porous Media, Elsevier, Amsterdam, 1992, pp. 327–336.
[12] L. Storesletten, Effects of anisotropy on convective flow through porous media, in: D.B. Ingham, I. Pop (Eds.), Transport Phenomena in Porous Media, Pergamon Press, Oxford, 1998, pp. 261–283.
[13] L. Storesletten, Effects of anisotropy on convection in horizontal and inclined porous layers, in: D.B. Ingham et al. (Eds.), Emerging Technologies and Techniques in Porous Media, Kluwer Academic Publishers, Netherlands, 2004, pp. 285–306.
[14] M.S. Malashetty, I.S. Shivakumara, K. Sridhar, The onset of convection in an anisotropic porous layer using a thermal non-equilibrium model, Transp. Porous Med. 60 (2005) 199–215.
[15] I.S. Shivakumara, Jinho Lee, A.L. Mamatha, M. Ravisha, Boundary and thermal non-equilibrium effects on convective instability in an anisotropic porous layer, J. Mech. Sci. Technol. 25 (4) (2011) 911–921.
[16] Y. Qin, P.N. Kaloni, Nonlinear stability problem of a rotating porous layer, Q. Appl. Math. 53 (1) (1995) 129–142.
[17] P. Vadasz, Coriolis effect on gravity-driven convection in a rotating porous layer heated from below, J. Fluid Mech. 376 (1998) 351–375.
[18] P. Vadasz, Flow and thermal convection in rotating porous media, in: K. Vafai (Ed.), Handbook of Porous Media, Marcel Dekker Inc, New York, 2000, pp. 395–440.
[19] B. Straughan, A sharp nonlinear stability threshold in rotating porous convection, Proc. R. Soc. London 457 (2001) 87–93.
[20] S. Govender, Coriolis effect on the linear stability of convection in a porous layer placed far away from the axis of rotation, Transp. Porous Med. 51 (2003) 315–326.
[21] M.S. Malashetty, Mahantesh Swamy, Sridhar Kulkarni, Thermal convection in a rotating porous layer using a thermal non equilibrium model, Phys. Fluids 19 (2007). 054102-1 054102-16.
[22] I.S. Shivakumara, M.N. Savitha, K.B. Chavaraddi, N. Devaraju, Bifurcation analysis for thermal convection in a rotating porous layer, Meccanica 44 (2009) 225–238.
[23] P. Falsaperla, G. Mulone, B. Straughan, Rotating porous convection with prescribed heat flux, Int. J. Eng. Sci. 48 (2010) 685–692.
[24] S. Govender, Coriolis effect on the stability of centrifugally driven convection in a rotating anisotropic porous layer subjected to gravity, Transp. Porous Med. 67 (2007) 219–227.
[25] S. Govender, P. Vadasz, The effect of mechanical and thermal anisotropy on the stability of gravity driven convection in rotating porous media in the presence of thermal non-equilibrium, Transp. Porous Med. 69 (2007) 55–66.
[26] E. Palm, A. Tyvand, Thermal convection in a rotating porous layer, J. Appl. Math. Phys. (ZAMP) 35 (1984) 122–123.
[27] J.F. Epherre, Criterion for the appearance of natural convection in an anisotropic porous layer, Int. J. Chem. Eng. (English translation) 17 (1975) 615–616.